Theory of mode coupling in a photorefractive crystal waveguide

Huang-Tzung Jan and Sien Chi

Institute of Electro-Optical Engineering, National Chiao Tung University, Hsinchu 30050, Taiwan

Pochi Yeh

Department of Electrical and Computer Engineering, University of California, Santa Barbara, California 93106

Received March 11, 1999

The mode coupling among guided modes in a photorefractive crystal waveguide is investigated. We derive the coupled equations of guided modes in a photorefractive crystal waveguide. Analytical solutions of the coupled equations are obtained for a two-mode photorefractive crystal waveguide. We also numerically analyze the coupled equations of guided modes in a multimode photorefractive crystal fiber. As a result of the coupling, power may flow to the fundamental mode or the highest-order mode, depending on the direction of the crystal optical axis. In addition, we report an analytical solution of the modal power in core and cladding for all guided $HE_{\nu m}$ and $EH_{\nu m}$ modes for cylindrical fibers made of uniaxial crystals. © 2000 Optical Society of America [S0740-3224(00)02406-1]

OCIS codes: 190.5330, 060.4370.

1. INTRODUCTION

Photoinduced fiber gratings in fibers can be produced by the transverse holographic method,[1] the point-to-point external writing,[2] or the internal modal interferometric process.[3] The presence of these gratings may cause coupling among the propagating modes.[2–4] It is known that a nonreciprocal energy coupling between optical beams exists in bulk photorefractive crystals (PRC's).[5,6] In this paper we investigate the nonreciprocal power transfer among the modes by means of the self-induced index grating. The wave function of these modes in a single-crystal fiber has been previously obtained.[7,8] In this paper we derive the coupled equations of guided modes in a PRC waveguide and solve the coupled equations of guided modes analytically in a two-mode PRC waveguide. We also numerically analyze the coupled equations of guided modes in a multimode PRC fiber. As a result of the coupling, power may flow to the fundamental mode or the highest-order mode, depending on the direction of the crystal optical axis relative to the propagation direction. We also report analytical solutions of the modal power in core and cladding for all guided HE and EH modes. Previous work had reported analytical results for TE and TM modes in cylindrical fibers made of uniaxial crystals.[8] To our knowledge, we are the first to report these analytical solutions for the hybrid modes.

2. FORMULATION OF THE PROBLEM

We consider a PRC waveguide, whose modes propagate along the crystal c axis. For the purpose of our derivation, the modal wave functions are normalized such that

$$\int_0^{2\pi}\int_0^{\infty} \mathbf{F}_i(r,\phi)\cdot\mathbf{F}_j^*(r,\phi)r\,dr\,d\phi = \delta_{ij},$$

where $\mathbf{F}_i(r,\phi)$ and $\mathbf{F}_j(r,\phi)$ are the modal wave functions of the waveguide. The total electric field in the PRC waveguide can be written as

$$\mathbf{E} = \sum_{j=1}^{n} A_j(z)\mathbf{F}_j(r,\phi)\exp(-i\beta_j z), \tag{1}$$

where β_j is a propagation constant and $A_j(z)$ is assumed to be a slowly varying mode amplitude. The summation is over all the propagating modes, $j = 1, 2, \ldots, n$. Within a factor of proportionality, the intensity of the electromagnetic radiation can be written as $I = |\mathbf{E}|^2$. Using Eq. (1) for the electric field, we can write the intensity as

$$I = I_0 + \sum_{j=1}^{n-1}\sum_{k=j+1}^{n}\{A_j(z)A_k^*(z)\mathbf{F}_j(r,\phi)\cdot\mathbf{F}_k^*(r,\phi) \times \exp[-i(\beta_j-\beta_k)z] + \text{c.c.}\}, \tag{2}$$

where $I_0 = \sum_{k=1}^{n}|A_k(z)\mathbf{F}_k(r,\phi)|^2$. The intensity I exhibits a spatial variation inside the PRC waveguide. Inside the PRC waveguide, such an intensity pattern will generate a spatial distribution of charge carriers. As a result, a space-charge field is created in the PRC waveguide. This field induces an index grating by means of the Pockels effect. In general, the index grating will have a spatial phase shift relative to the interference pattern. The dielectric tensor of the photoinduced gratings can be written as[9]

$$\epsilon' = \epsilon + \sum_{j=1}^{n-1}\sum_{k=j+1}^{n}\frac{(\Delta\epsilon)_{jk}}{(I_{\text{avg}})_{jk}}\{A_j(z)A_k^*(z)\mathbf{F}_j(r,\phi) \cdot \mathbf{F}_k^*(r,\phi)\exp[-i(\beta_j-\beta_k)z]\exp(i\Phi) + \text{c.c.}\}, \tag{3}$$

where ϵ is the dielectric tensor of the fiber when no light is present, $(\Delta\epsilon)_{jk}$ is the photoinduced dielectric modula-

0740-3224/2000/071176-06$15.00

tion depth tensor between the jth and kth modes, Φ is a spatial phase shift between the index grating and the interference pattern, and

$$(I_{\mathrm{avg}})_{jk} = \frac{\sum_{j=1}^{n} \int_0^{2\pi} \int_0^{\infty} |\mathbf{E}_j|^2 r \mathrm{d}r \mathrm{d}\phi}{(A_{\mathrm{eff}})_{jk}} = \frac{\sum_{j=1}^{n} A_j A_j^*}{(A_{\mathrm{eff}})_{jk}}, \quad (4)$$

with $(A_{\mathrm{eff}})_{jk}$ being the modal field overlap area between the jth and kth modes of the waveguide[10]:

$$(A_{\mathrm{eff}})_{ij} = \frac{\int_0^{2\pi} \int_0^{\infty} |\mathbf{F}_i(r,\phi)|^2 r \mathrm{d}r \mathrm{d}\phi \int_0^{2\pi} \int_0^{\infty} |\mathbf{F}_j(r,\phi)|^2 r \mathrm{d}r \mathrm{d}\phi}{\int_0^{2\pi} \int_0^{\infty} |\mathbf{F}_i(r,\phi)|^2 |\mathbf{F}_j(r,\phi)|^2 r \mathrm{d}r \mathrm{d}\phi}$$

$$= \frac{1}{\int_0^{2\pi} \int_0^{\infty} |\mathbf{F}_i(r,\phi)|^2 |\mathbf{F}_j(r,\phi)|^2 r \mathrm{d}r \mathrm{d}\phi}. \quad (5)$$

Equation (3) represents a photorefractive index grating in the crystal waveguide formally identical to those of the bulk crystals. If the medium is isotropic, the equation of the photoinduced index grating can be simplified to

$$n' = n_0 + \sum_{i=1}^{n-1} \sum_{j=i+1}^{n} \Delta n_{ij} [\exp(-iK_{ij}z) \exp(i\Phi) + \mathrm{c.c.}], \quad (3')$$

where Δn_{ij} is the photoinduced index modulation depth between the jth and kth modes, z is the distance measurement along the axis of the fiber, and K_{ij} is the difference between the propagation constants ($K_{ij} = \beta_i - \beta_j$). This grating is a transmission grating. Mode i with propagation constant β_i is scattered into mode j with $\beta_j = \beta_i - K_{ij}$, and mode j with propagation constant β_j is scattered into mode i with $\beta_i = \beta_j + K_{ij}$. There is some transverse variation of the photoinduced index grating that is due to the transverse variation of the wave functions of the modes. Since the space-charge field is along the c axis, the photoinduced dielectric modulation depth tensor $\Delta\epsilon$ can be written as[9]

$$\Delta\epsilon = -\frac{1}{\epsilon_0} \epsilon \begin{bmatrix} r_{13} & r_{63} & r_{53} \\ r_{63} & r_{23} & r_{43} \\ r_{53} & r_{43} & r_{33} \end{bmatrix} \epsilon E_0^{\mathrm{SC}}, \quad (6)$$

with

$$E_0^{\mathrm{SC}} = \frac{E_d E_q}{E_d + E_q} \left[\frac{1 + \left(\frac{E_0}{E_d} \right)^2}{1 + \left(\frac{E_0}{E_d + E_q} \right)^2} \right]^{1/2}, \quad (7)$$

where E_0 is an externally applied electric field, $E_q = eN_A/K\epsilon_3$, $E_d = K(k_B T/e)$, ϵ is the dielectric tensor, and $K = |\beta_i - \beta_j|$ is the magnitude of the grating wave vector for the index grating formed by modes i and j. For crystals such as SBN and $LiNbO_3$, the electro-optic coefficients $r_{43} = r_{53} = r_{63} = 0$, and $\Delta\epsilon$ becomes a diagonal tensor:

$$\Delta\epsilon = -\frac{1}{\epsilon_0} \begin{bmatrix} r_{13} n_o^4 & 0 & 0 \\ 0 & r_{23} n_o^4 & 0 \\ 0 & 0 & r_{33} n_e^4 \end{bmatrix} E_0^{\mathrm{SC}}. \quad (8)$$

The phase $\Phi = \pi/2 + \tan^{-1}\{E_0 E_q / [E_0^2 + E_d(E_d + E_q)]\}$ indicates the degree to which the index grating is shifted spatially with respect to the light interference pattern. In PRC waveguides that operate by diffusion only, with no applied electric field, for example SBN, the magnitude of Φ is $\pi/2$, with its sign depending on the direction of the c axis. The presence of such a phase shift allows the possibility of a nonreciprocal steady-state transfer of power among waveguide modes. The parameter $\Delta\epsilon$ depends on the material properties of the crystal (electro-optic coefficient) and the period of the photoinduced grating.

To investigate the coupling, we substitute Eqs. (3) and (8) for the dielectric tensor ϵ' and Eq. (1) for the electric field into the following wave equation:

$$\nabla^2 \mathbf{E} + \frac{\omega^2}{c^2} \frac{\epsilon'}{\epsilon_0} \mathbf{E} = 0, \quad (9)$$

where c is the velocity of light in vacuum and ω is the angular frequency of light. Using the slowly varying amplitude approximation, that is,

$$\left| \frac{\mathrm{d}^2}{\mathrm{d}z^2} A_j \right| \ll \left| \beta_j \frac{\mathrm{d}}{\mathrm{d}z} A_j \right|, \qquad j = 1, \ldots, n, \quad (10)$$

we obtain

$$\sum_{j=1}^{n} 2i\beta_j \frac{\mathrm{d}A_j(z)}{\mathrm{d}z} \mathbf{F}_j \exp(-i\beta_j z)$$

$$= \sum_{j=1}^{n} \sum_{k=j+1}^{n} \frac{\omega^2 (\Delta\epsilon)_{jk} (A_{\mathrm{eff}})_{jk}}{2c^2 \epsilon_0 \sum_{l=1}^{n} A_l A_l^*} \{ \mathbf{F}_j^* \cdot \mathbf{F}_k \mathbf{F}_j A_j A_j^* A_k$$

$$\times \exp(-i\beta_k z + i\Phi) + \mathbf{F}_j \cdot \mathbf{F}_k^* \mathbf{F}_k A_j A_k A_k^*$$

$$\times \exp(-i\beta_j z - i\Phi) + \mathbf{F}_j^* \cdot \mathbf{F}_k \mathbf{F}_k A_j^* A_k A_k$$

$$\times \exp[-i(2\beta_k - \beta_j)z + i\Phi] + \mathbf{F}_j$$

$$\cdot \mathbf{F}_k^* \mathbf{F}_j A_j A_j A_k^* \exp[i(\beta_k - 2\beta_j)z - i\Phi] \}. \quad (11)$$

Next, using the orthogonality of modal wave functions and neglecting fast-varying phase terms, we obtain the following coupled equations:

$$\frac{\mathrm{d}A_j(z)}{\mathrm{d}z} = \sum_{k=1}^{n} (1 - \delta_{jk})$$

$$\times \frac{\omega^2 (A_{\mathrm{eff}})_{jk}}{4ic^2 \epsilon_0 \beta_j} \langle \mathbf{F}_j^* \cdot \mathbf{F}_k \mathbf{F}_k^* \cdot (\Delta\epsilon)_{jk} \mathbf{F}_j \rangle$$

$$\times \exp[\mathrm{sign}(j-k) i\Phi] \frac{A_j A_k A_k^*}{\sum_{l=1}^{n} A_l A_l^*} - \frac{\alpha}{2} A_j, \quad (12)$$

where we have added terms that account for the attenuation with α as the PRC fiber absorption coefficient and

$$\langle \mathbf{F}_j \cdot \mathbf{F}_k^* \mathbf{F}_j^* \cdot (\Delta\epsilon)_{jk} \mathbf{F}_k \rangle = \int_0^{2\pi} \int_0^{\infty} \mathbf{F}_j \cdot \mathbf{F}_k^* \mathbf{F}_j^* \cdot (\Delta\epsilon)_{jk} \mathbf{F}_k r \, \mathrm{d}r \, \mathrm{d}\phi.$$

We now write

$$A_j(z) = \sqrt{M_j(z)} \exp[i\Psi_j(z)], \tag{13}$$

where $M_j(z)$ and $\Psi_j(z)$ are the modulus and the phase of the complex amplitude $A_j(z)$. With the use of Eq. (13), the coupled equations (12) can be written as

$$\frac{\mathrm{d}M_j(z)}{\mathrm{d}z} = \sum_{k=1}^{n} \mathrm{sign}(j-k)\gamma_{jk} \frac{M_j(z)M_k(z)}{\sum_{l=1}^{n} M_l(z)} - \alpha M_j, \qquad j = 1, \ldots, n, \tag{14}$$

$$\frac{\mathrm{d}}{\mathrm{d}z}\Psi_j(z) = \sum_{k=1}^{n} \sigma_{jk} \frac{M_k(z)}{\sum_{l=1}^{n} M_l(z)}, \qquad j = 1, \ldots, n, \tag{15}$$

where

$$\gamma_{jk} = (1-\delta_{jk}) \frac{\omega^2 (A_{\mathrm{eff}})_{jk}}{2c^2 \epsilon_0 \beta_j} \times \langle \mathbf{F}_j \cdot \mathbf{F}_k^* \mathbf{F}_j^* \cdot (\Delta\epsilon)_{jk} \mathbf{F}_k \rangle \sin(\Phi), \tag{16}$$

$$\sigma_{jk} = (1-\delta_{jk}) \frac{\omega^2 (A_{\mathrm{eff}})_{jk}}{4c^2 \epsilon_0 \beta_j} \times \langle \mathbf{F}_j \cdot \mathbf{F}_k^* \mathbf{F}_j^* \cdot (\Delta\epsilon)_{jk} \mathbf{F}_k \rangle \cos(\Phi). \tag{17}$$

In waveguides, components of the modal wave functions are always real or imaginary, and $(\Delta\epsilon)_{jk} = (\Delta\epsilon)_{kj}$. Thus we obtain $\mathbf{F}_j \cdot \mathbf{F}_k^* \mathbf{F}_j^* \cdot (\Delta\epsilon)_{jk} \mathbf{F}_k = \mathbf{F}_k \cdot \mathbf{F}_j^* \mathbf{F}_k^* \cdot (\Delta\epsilon)_{jk} \mathbf{F}_j$. We note that $\beta_j \gamma_{jk} = \beta_k \gamma_{kj}$ for any two modes. According to Eq. (14), it can be shown that the total power flow, which is proportional to $\Sigma_{j=1}^{n} \beta_j M_j(z)$, is a constant when $\alpha = 0$. In the absence of material absorption ($\alpha = 0$), $M_1(z)$ is an increasing function provided that $\gamma_{1k} \leqslant 0$ for all $k > 1$. This indicates that the power is flowing into the lowest-order mode. On the other hand, $M_n(z)$ is an increasing function provided that $0 \leqslant \gamma_{nk}$ for all $k < n$. The sign of γ_{jk} determines the direction of power flow, which depends on the orientation of the crystal axis. In PRC waveguides that operate by diffusion only (i.e., no external static field), for example SBN, the magnitude of Φ is $\pi/2$, with a sign depending on the orientation of the crystal optical axis relative to the propagation direction.

3. EXAMPLES OF PHOTOREFRACTIVE CRYSTAL FIBERS

For illustration purposes we consider some PRC fibers with a core of uniaxial crystal (with refractive indices n_{o1} and n_{e1}) and a cladding of uniaxial crystal or an isotropic medium (with refractive indices n_{o2} and n_{e2} or n_2, respectively). A step-index profile is assumed, and the crystal c axis is parallel to the axis of the fibers. In this case it can be shown that the V number of the fiber is the same as that of the step-index-profile isotropic-medium fiber. In other words, $V = (2\pi a/\lambda)(n_{o1}^2 - n_{o2}^2)^{1/2}$ or $(2\pi a/\lambda)(n_{o1}^2 - n_2^2)^{1/2}$. Modal parameters U and W for core and cladding are defined by $U = a(k^2 n_{o1}^2 - \beta^2)^{1/2}$ and $W = a(\beta^2 - k^2 n_{o2}^2)^{1/2}$, where $k = 2\pi/\lambda$ with wavelength λ, a is the core radius, and β is the modal propagation constant. Cutoff conditions of the uniaxial fiber were previously reported.[7] Dai and Jen[8] had reported modal fields for the uniaxial core–uniaxial cladding crystal fiber and also expressed the modal powers of the TE and TM modes in closed form. In this paper we report the closed-form solutions of the modal powers of HE and EH modes in uniaxial crystal fibers. The $\mathrm{HE}_{\nu m}$ and $\mathrm{EH}_{\nu m}$ modal powers in the core and cladding regions can be written, respectively, as

$$P_{\mathrm{co}} = \frac{\pi a^2}{2} \left(\frac{\epsilon_0}{\mu_0}\right)^{1/2} \frac{\beta}{k} \left\{ \frac{\kappa_{\mathrm{co}}^2 k^2 n_{o1}^2}{2\beta^2} \left[\frac{J_{\nu-1}^2(\kappa_{\mathrm{co}} U)}{J_\nu^2(\kappa_{\mathrm{co}} U)} - \frac{J_{\nu-2}(\kappa_{\mathrm{co}} U)}{J_\nu(\kappa_{\mathrm{co}} U)} \right] + \frac{F_2^2}{2} \left[\frac{J_{\nu-1}^2(U)}{J_\nu^2(U)} - \frac{J_{\nu-2}(U)}{J_\nu(U)} \right] - \frac{\nu}{U^2}(1+F_2) \left(\frac{k^2 n_{o1}^2}{2\beta^2} + F_2 \right) \right\}, \tag{18}$$

$$P_{\mathrm{cl}} = \frac{\pi a^2}{2} \left(\frac{\epsilon_0}{\mu_0}\right)^{1/2} \frac{\beta}{k} \left(\frac{U}{W}\right)^2 \left\{ \frac{\kappa_{\mathrm{cl}}^2 k^2 n_{o2}^2}{2\beta^2} \left[\frac{K_{\nu-2}(\kappa_{\mathrm{cl}} W)}{K_\nu(\kappa_{\mathrm{cl}} W)} - \frac{K_{\nu-1}^2(\kappa_{\mathrm{cl}} W)}{K_\nu^2(\kappa_{\mathrm{cl}} W)} \right] + \frac{F_2^2}{2} \left[\frac{K_{\nu-2}(W)}{K_\nu(W)} - \frac{K_{\nu-1}^2(W)}{K_\nu^2(W)} \right] + \frac{\nu}{W^2}(1-F_2) \left(\frac{k^2 n_{o2}^2}{2\beta^2} - F_2 \right) \right\}, \tag{19}$$

where

$$F_2 = \left(\frac{V}{UW}\right)^2 \frac{\nu}{\frac{1}{2U}\left[\frac{J_{\nu-1}(U)}{J_\nu(U)} - \frac{J_{\nu+1}(U)}{J_\nu(U)}\right] - \frac{1}{2W}\left[\frac{K_{\nu-1}(W)}{K_\nu(W)} + \frac{J_{\nu+1}(W)}{J_\nu(W)}\right]}.$$

$\kappa_{\mathrm{co}} = n_{e1}/n_{o1}$ and $\kappa_{\mathrm{cl}} = n_{e2}/n_{o2}$ are index ratios between the e ray and the o ray of the PRC fiber in core and cladding.

Table 1 shows the cutoff conditions (minimum V num-

Table 1. Cutoff Values of *V* Number

Mode	(1) $n_{cl} = 1$	(2) $n_{cl} = 1.45$	(3) $n_{cl}^{t} = 2.346$, $n_{cl}^{z} = 2.31$
HE_{11}	0	0	0
TE_{01}	2.404826	2.404826	2.404826
HE_{21}	3.277405	2.8926845	2.42447
TM_{01}	2.496311	2.496311	2.4356962
EH_{11}	3.831706	3.831706	3.831706
HE_{31}	4.7534085	4.3963371	3.8615067
HE_{12}	3.977474	3.977474	3.8808935
HE_{41}	6.0751014	5.73888	5.174301
EH_{21}	5.145449	5.1528398	5.1660751
TE_{02}	5.520078	5.520078	5.5200781
HE_{22}	6.1823798	5.8333314	5.5598849
TM_{02}	5.730076	5.730076	5.5909392
EH_{31}	6.3926285	6.4020849	6.4190246

bers) of the first 13 modes for three examples: (1) a SBN:60 rod[11] with $n_{o1} = 2.367$ and $n_{e1} = 2.337$, (2) a SBN:60 core with a silica glass cladding, and (3) a SBN:60 core with Ce-doped SBN:60 cladding[11] with $n_{o2} = 2.346$ and $n_{e2} = 2.310$.

4. SOLUTION OF THE TWO-MODE COUPLING

If a PRC fiber has a cutoff between the TE_{01} and HE_{21} modes, then there are only two guided modes (HE_{11} and TE_{01}) in this fiber. The modal intensity can be analytically solved. The solutions of the two-mode PRC fiber can be written as

$$M_1(z)[c_0 - \beta_1 M_1(z)]^{-1/r} = M_1(0)[c_0 - \beta_1 M_1(0)]^{-1/r}\exp(-\gamma_1 z), \quad (20)$$

$$M_2(z)[c_0 - \beta_2 M_2(z)]^{-r} = M_2(0)[c_0 - \beta_2 M_2(0)]^{-r}\exp(\gamma_2 z), \quad (21)$$

where

$$\gamma_1 = \frac{\omega^2 (A_{\text{eff}})_{12}}{2c^2\epsilon_0\beta_1}\langle \mathbf{F}_2 \cdot \mathbf{F}_1^* \mathbf{F}_2^* \cdot (\Delta\epsilon)_{12}\mathbf{F}_1\rangle \sin(\Phi),$$

$$\gamma_2 = \frac{\omega^2 (A_{\text{eff}})_{21}}{2c^2\epsilon_0\beta_2}\langle \mathbf{F}_1 \cdot \mathbf{F}_2^* \mathbf{F}_1^* \cdot (\Delta\epsilon)_{21}\mathbf{F}_2\rangle \sin(\Phi),$$

$r = \beta_2/\beta_1$, and $c_0 = \beta_1 M_1(0) + \beta_2 M_2(0)$. Here the subscripts 1 and 2 stand for modes HE_{11} and TE_{01}, respectively. Note that, in the presence of material absorption ($\alpha > 0$), the solutions can be modified as

$$M_j^{\alpha}(z) = M_j(z)\exp(-\alpha z). \quad (22)$$

With $M_1(z)$ and $M_2(z)$ known, the phases $\Psi_1(z)$ and $\Psi_2(z)$ can be obtained by integrating Eq. (15). Using Eq. (14), we obtain

$$\Psi_j(z) - \Psi_j(0) = (-1)^j \frac{\cot(\Phi)}{2}\ln\left[\frac{M_j(z)}{M_j(0)}\right], \quad j = \text{HE}_{11} \text{ or } \text{TE}_{01}. \quad (23)$$

If $\Phi = \pi/2$, we note that phases are constant (independent of z).

These results are similar to those of two-wave mixing in bulk PRC's. For SBN PRC fibers that operate by diffusion only (i.e., no external static field), the magnitude of Φ is $\pi/2$, with a sign depending on the orientation of the c axis. By examining Eqs. (20) and (21), we find that the direction of power flow is determined by the sign of $\gamma_{HE_{11}}$ or $\gamma_{TE_{01}}$, which depends on the orientation of the crystal c axis. In the absence of material absorption ($\alpha = 0$), $M_{HE_{11}}(z)$ is an increasing function of z provided that $\gamma_{HE_{11}}$ is negative. This indicates that the power is flowing from the higher-order mode TE_{01} to the fundamental mode HE_{11} in a two-mode photorefractive fiber.

5. NUMERICAL RESULTS FOR MULTIMODE COUPLING

We consider a ten-mode PRC uniaxial SBN rod, with $V = 5.74$, $\lambda = 0.5145\,\mu$m, and dopant density $N_D = 2N_A = 10^{17}\,\text{cm}^{-3}$. The propagation constants of the guided modes are shown in Table 2 in units of ω/c.

By examining the coupled Equations (14), we note that the power transfer rate is proportional to γ_{jk}. According to Eq. (16), we can rewrite the coupling constant such that

$$\gamma_{jk} = (1 - \delta_{jk})\frac{\omega^2}{2c^2\epsilon_0\beta_j} f_{jk}(E_0^{\text{SC}})_{jk}, \quad (24)$$

where

$$f_{jk} = -\frac{\oint \mathbf{F}_j \cdot \mathbf{F}_k^* \mathbf{F}_j^* \cdot \begin{bmatrix} r_{13}n_o^4 & 0 & 0 \\ 0 & r_{13}n_o^4 & 0 \\ 0 & 0 & r_{33}n_e^4 \end{bmatrix} \mathbf{F}_k \, da}{\oint \mathbf{F}_j \cdot \mathbf{F}_j^* \mathbf{F}_k^* \cdot \mathbf{F}_k \, da}$$

is the modal field factor, with r_{jk} being the element of the electro-optic tensor, and $(E_0^{\text{SC}})_{jk}$ is the space-charge field, which depends on the period of the jth and kth modes' photoinduced grating and the SBN impurity dopant density.[6] In this example we have $(E_0^{\text{SC}})_{jk} = (E_0^{\text{SC}})_{kj}$ and $f_{jk} = f_{kj}$. Figure 1 shows the SBN space-charge field as a function of the photoinduced grating period for two dopant densities, $N_D = 10^{17}$ and $10^{16}\,\text{cm}^{-3}$. When the grating period $\Lambda_G = 1.409\,\mu$m and the dopant density $N_D = 2N_A = 10^{17}\,\text{cm}^{-3}$, the SBN samples have a maximum space-charge field $E_0^{\text{SC}} \approx 5.4 \times 10^4$ V/m.

The upper-triangular half of Table 3 shows $f_{jk}/r_{13}n_o^4$, which displays the difference between the bulk and the waveguide medium (for the bulk medium, this factor is unity). The modal field factor is zero between the TE and TM modes because $\mathbf{F}_{\text{TE}} \cdot \mathbf{F}_{\text{TM}} = 0$. We note that a maximum value of the modal field factor is produced by the TE_{01} and TE_{02} modes and that a minimum value is

Table 2. Propagation Constants of SBN Rod

Mode	$\beta\,(\omega/c)$
HE_{11}	2.21629
TE_{01}	2.03486
HE_{21}	1.95544
TM_{01}	1.91723
EH_{11}	1.70497
HE_{31}	1.53337
HE_{12}	1.39819
EH_{21}	1.26314
TE_{02}	1.07166
TM_{02}	1.00701

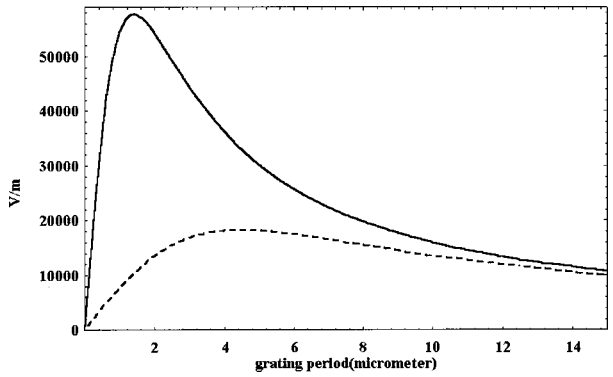

Fig. 1. SBN space-charge field as function of the photoinduced grating wavelength for two doped densities: $N_D = 10^{17}\,\mathrm{cm}^{-3}$ (solid curve) and $N_D = 10^{16}\,\mathrm{cm}^{-3}$ (dashed curve).

produced by the EH_{11} and TM_{02} modes. The variation is a result of the overlap integral of the modal field profiles. The lower-triangular half of Table 3 shows the photoinduced grating period $(\Lambda_G)_{jk} = (\Lambda_G)_{kj}$ between any two modes of the fiber in units of micrometers. According to the grating periods and Fig. 1, we note that the space-charge fields are in the range between 1.2×10^4 and 5.8×10^4 V/m.

Table 4 shows the photorefractive coupling constants γ_{jk} between any two modes of this ten-mode fiber. We note that coupling constants $\gamma_{\mathrm{TE,TM}} = 0$ between the TE and TM modes because their wave functions are orthogonal: $\mathbf{F}_{\mathrm{TE}} \cdot \mathbf{F}_{\mathrm{TM}} = 0$. A slight difference between γ_{jk} and γ_{kj} is a result of the difference in β_j and β_k (we recall that $\beta_j \gamma_{jk} = \beta_k \gamma_{kj}$). According to our numerical analysis, we find that modal wave-function contributions are more significant than those of the space-charge fields. We also note that the coupling constant between the HE_{31} and HE_{21} modes is maximum because they have a higher modal field factor and a higher space-charge field.

Figure 2 shows the modal power as functions of z for $\Phi = -\pi/2$. In the absence of absorption, we note that $P_{\mathrm{HE}_{11}}$ is an increasing function of z in the fiber. We also note that the HE_{11} mode will gain virtually all the power in a few centimeters. Three low-order modes, TE_{01}, HE_{21}, and TM_{01}, initially gain the power from higher-order modes but eventually donate all the power to the fundamental mode HE_{11}. All other modes are decreasing functions of z [see Fig. 2(b)]. On the other hand, when

Table 3. $f_{jk}/r_{13}n_o^4$ Factors[a] and Grating Periods $(\Lambda_G)_{jk}$[b]

	HE_{11}	TE_{01}	HE_{21}	TM_{01}	EH_{11}	HE_{31}	HE_{12}	EH_{21}	TE_{02}	TM_{02}
HE_{11}	*	0.5002	0.6526	0.3156	0.4677	0.7221	0.2718	0.3871	0.4897	0.1087
TE_{01}	2.836	*	0.4455	0	0.6431	0.3340	0.0910	0.3723	0.9580	0
HE_{21}	1.972	6.479	*	0.3562	0.4455	0.8390	0.2394	0.3712	0.4141	0.1406
TM_{01}	1.72	4.374	13.46	*	0.1624	0.2962	0.3542	0.2995	0	0.3895
EH_{11}	1.006	1.56	2.054	2.424	*	0.3515	0.1313	0.6385	0.4200	0.0402
HE_{31}	0.7534	1.026	1.219	1.34	2.998	*	0.2547	0.3135	0.2482	0.1421
HE_{12}	0.6289	0.8081	0.9233	0.9913	1.677	3.806	*	0.1624	0.1227	0.1619
EH_{21}	0.5398	0.6667	0.7432	0.7866	1.164	1.904	3.81	*	0.3506	0.0625
TE_{02}	0.4495	0.5342	0.5822	0.6085	0.8124	1.114	1.576	2.687	*	0
TM_{02}	0.4255	0.5006	0.5425	0.5652	0.7371	0.9775	1.315	2.009	7.958	*

[a] Upper-triangular half of the table.
[b] Lower-triangular half of the table, in units of micrometers.

Table 4. Coupling Constants[a]

	HE_{11}	TE_{01}	HE_{21}	TM_{01}	EH_{11}	HE_{31}	HE_{12}	EH_{21}	TE_{02}	TM_{02}
HE_{11}	*	109.3	263.9	110.3	128.4	311.0	88.52	71.42	77.75	30.87
TE_{01}	119.1	*	55.25	0	191.1	94.93	23.45	85.97	189.6	0
HE_{21}	299.2	57.50	*	31.31	154.7	560.1	142.3	117.3	90.82	80.34
TM_{01}	127.5	0	31.93	*	20.40	150.7	294.9	58.03	0	274.1
EH_{11}	166.9	228.0	177.4	22.94	*	128.0	55.18	274.6	129.5	16.79
HE_{31}	449.5	126.0	714.3	188.5	142.3	*	169.2	180.0	95.72	175.7
HE_{12}	140.3	34.12	199.9	404.4	67.28	185.6	*	82.20	53.00	228.5
EH_{21}	125.3	138.5	181.6	88.07	370.7	218.5	90.99	*	138.8	64.42
TE_{02}	160.8	360.1	165.7	0	206.1	137.0	69.14	163.6	*	0
TM_{02}	67.95	0	156.0	521.9	28.43	267.5	317.3	80.81	0	*

[a] In units of micrometers.

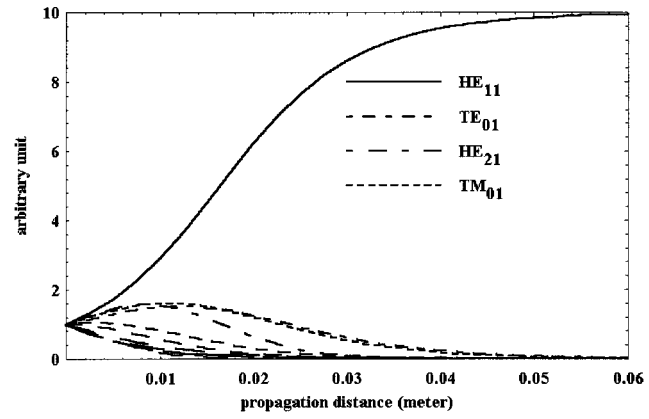

(a)

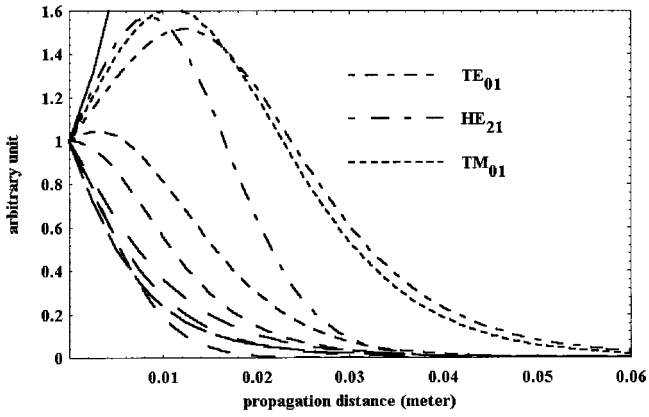

(b)

Fig. 2. Modal power versus propagation distance for ten-mode SBN rod with $\Phi = -\pi/2$ and $\gamma_{1k} < 0$.

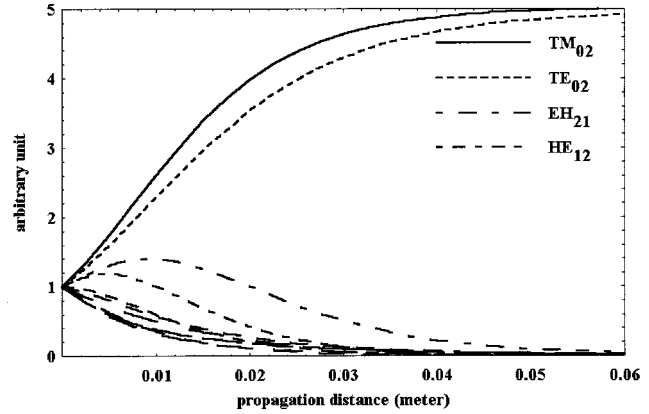

Fig. 3. Modal power versus propagation distance for ten-mode SBN rod with $\Phi = +\pi/2$ and $\gamma_{1k} > 0$.

the direction of the c axis is reversed and the propagation direction remains the same, the coupling coefficients reverse their signs.[12] In this case the two highest modes, TE_{02} and TM_{02}, will gain the power. Figure 3 shows the modal power as functions of z for $\Phi = +\pi/2$. There is no coupling between the TE_{02} and TM_{02} modes because their wave functions are orthogonal: $\mathbf{F}_{TE_{02}} \cdot \mathbf{F}_{TM_{02}} = 0$.

6. CONCLUSION

A complete analysis for the mode coupling among guided modes in a photorefractive crystal PRC waveguide is investigated, and the coupled equations in a two-mode PRC waveguide are analytically solved. A numerical analysis for the coupled equations of guided modes in a ten-mode PRC fiber is also presented. Based on the above analysis, we find that the power in a multimode waveguide can flow either to the fundamental mode or to the highest-order mode, depending on the direction of the crystal optical axis. Thus a PRC fiber can function like a mode converter. Such a PRC mode converter can also be employed to eliminate the fan-in power loss in an optical interconnection.[13]

ACKNOWLEDGMENT

This work was partially supported by the National Science Council, Republic of China, under contract NSC 88-2215-E-009-006.

Address correspondence to Sien Chi at the location on the title page or by phone, 886-3-5712121, ext 56324; fax, 886-3-5716631; or e-mail, schi@cc.nctu.edu.tw.

REFERENCES

1. G. Meltz, W. W. Morsey, and W. H. Gleen, "Formation of Bragg grating in optical fibers by a transverse holographic method," Opt. Lett. **14**, 823–825 (1989).
2. K. O. Hill, B. Malo, K. A. Vineberg, F. Bilodeau, D. C. Johnson, and I. Skinner, "Efficient mode conversion in telecommunication fibre using externally written gratings," Electron. Lett. **26**, 1270–1272 (1990).
3. H. G. Park and B. Y. Kim, "Intermodal coupler using permanently photoinduced grating in two-mode optical fibre," Electron. Lett. **25**, 797–799 (1989).
4. C. Shi and T. Okoshi, "Analysis of fiber-optic $LP_{01} \leftrightarrow LP_{02}$ mode converter," Opt. Lett. **17**, 719–721 (1992).
5. L. Solymar, "Theory of volume holographic formation in photorefractive crystal," in *Electro-Optic and Photorefractive Materials*, P. Gunter, ed. (Springer-Verlag, Berlin, 1987), Chap. 3, pp. 75–97.
6. P. Yeh, *Introduction to Photorefractive Nonlinear Optics* (Wiley, New York, 1993), Chap. 4, pp. 118–182.
7. A. Tonning, "Circularly symmetric optical waveguide with strong anisotropy," IEEE Trans. Microwave Theory Tech. **MTT-30**, 790–794 (1982).
8. J. D. Dai and C. K. Jen, "Analysis of cladded uniaxial single-crystal fibers," J. Opt. Soc. Am. A **8**, 2021–2025 (1991).
9. P. Yeh, "Two-wave mixing in nonlinear media," IEEE J. Quantum Electron. **25**, 484–519 (1989).
10. G. P. Agrawal, *Nonlinear Fiber Optics* (Academic, San Diego, Calif., 1989), Chap. 7, pp. 173–177.
11. G. L. Wood, W. W. Clark III, M. J. Miller, E. J. Sharp, G. J. Salamo, and R. R. Neurgaonkar, "Broadband photorefractive properties of self-pumped phase conjugation in Ce-SBN:60," IEEE J. Quantum Electron. **QE-23**, 2126–2135 (1987).
12. L. Li, K. G. Chittibabu, Z. Chen, J. I. Chen, S. Marturunkakul, J. Kumar, and S. K. Tripathy, "Photorefractive effect in a conjugated polymer based material," Opt. Commun. **152**, 257–261 (1996).
13. P. Yeh, "Reconfigurable optical interconnection," in *Integrated Optoelectronics for Communication and Processing*, C. S. Hong, ed., Proc. SPIE **1582**, 3–13 (1991).